

Disturbance Observer Application for the Compensation of the Phase Drift of the LANSCE DTL LINAC Solid State Power Amplifier

Sungil Kwon (skwon@lanl.gov), A. Archuleta, L. Castellano, J. Lyles, Colton Marchwinski, M. Prokop, P. Van Rooy, P. Torrez

Los Alamos National Laboratory, Los Alamos, NM, USA

I. Overall Control System Block Diagram

PI feedback Controller $C(s)$ and Disturbance Observer are implemented. PI feedback Controller is the default Controller. Disturbance Observer (DOB) is implemented to estimate the phase drift at 20kW Solid State Amplifier (SSA) which is treated as an input disturbance.

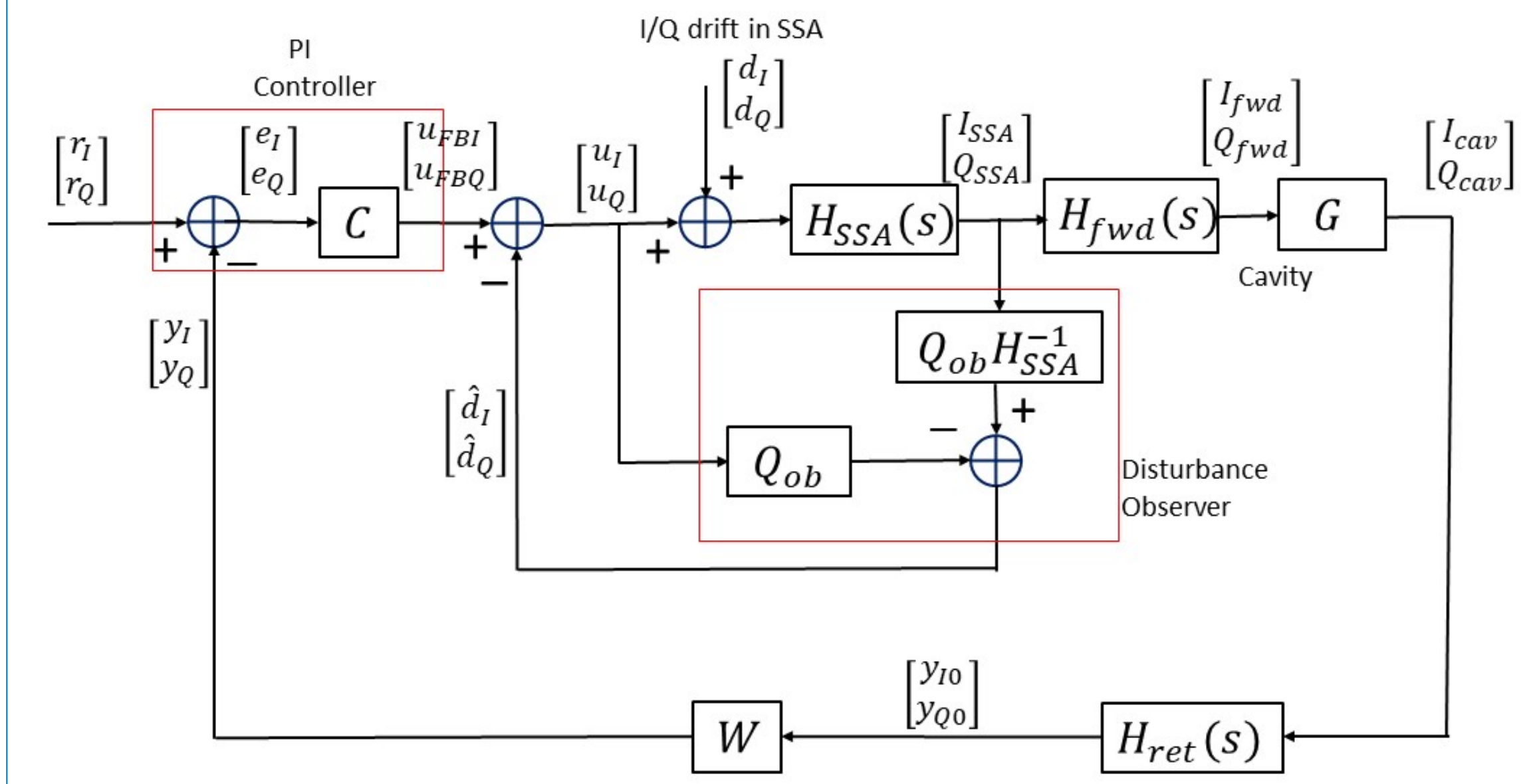


Figure 1. Overall LLRF Control System

II. Baseband Uncertainty Model of RF System

The accelerator RF cavity is modelled as two-input-two-output (TITO) uncertain system. The high power RF amplifier at an operating In-phase(I) and Quadrature(Q) points can be modelled with a gain and two-by-two phase rotation matrix. The cavity RF pickup loop also can be modelled with a gain and two-by-two phase rotation matrix. Hence, overall RF system can be described as a perturbed system $G_p(s)$ with the multiplicative uncertainty $\Delta(s, \Delta\omega)$ and shaping filter $M(s)$.

Perturbed Plant: $G_p(s) = G_n(s)(I + \Delta(s, \Delta\omega)M(s))$

Nominal Plant: $G_n(s) = \frac{h}{\tau_p s + 1} \begin{bmatrix} \cos(\theta) & -\sin(\theta) \\ \sin(\theta) & \cos(\theta) \end{bmatrix}$

$$\Delta(s, \Delta\omega) = \frac{1}{D(s, \Delta\omega)} \begin{bmatrix} -\left(\frac{\Delta\omega}{\omega_{3dB}}\right)^2 & -\frac{\Delta\omega}{\omega_{3dB}}(\tau_p s + 1) \\ \frac{\Delta\omega}{\omega_{3dB}}(\tau_p s + 1) & -\left(\frac{\Delta\omega}{\omega_{3dB}}\right)^2 \end{bmatrix}$$

$$D(s, \Delta\omega) = (\tau_p s + 1)^2 + \left(\frac{\Delta\omega}{\omega_{3dB}}\right)^2$$

$$\|\Delta(j\omega, \Delta\omega)\|_\infty < 1, \quad \|\Delta(j\omega, \Delta\omega)\|_\infty < \|M(j\omega)\|_\infty$$

h : Steady State Loop Gain

τ_p : Time Constant

θ : Overall Loop Phase Rotation

$\Delta\omega$: Detuning Frequency(rad/sec)

ω_{3dB} : cavity 3dB bandwidth(rad/sec)

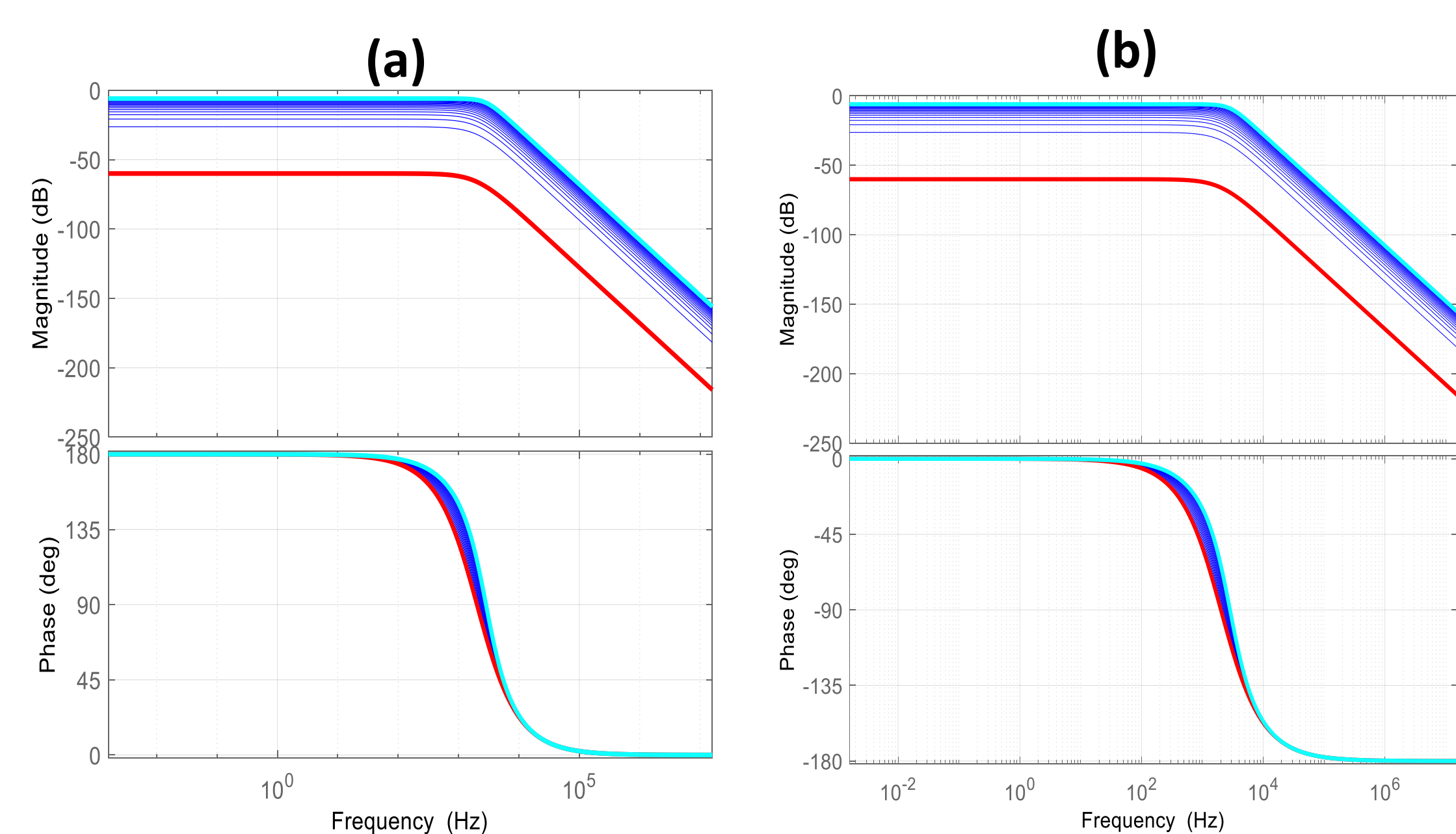


Figure 2. Bode Plots of the perturbed system: (a) u_Q to y_I ; (c) u_Q to y_I . The 3 dB bandwidth of the cavity is 1013 Hz. The detuning frequency range for investigation is from 20 Hz to 1013 Hz. Red line: $\Delta f = 20$ Hz. Cyan line: $\Delta f = 1013$ Hz.

III. Decoupling Controller

A simple intuitive approach to control the TITO multivariate system is described as a two-step procedure where a multivariate decoupling controller is designed to minimize with the off-diagonal cross-talk in $G_n(s)$, and then two, single-input single-output (SISO) controllers are designed and applied to each channel of the TITO system. A decoupling controller of the TITO system is a post-compensator, $W(s)$ that produces a newly shaped plant function $G_p(s)$. In the LANSCE Digital LLRF system, an adaptive gain and phase calibration is implemented on the LLRF FPGA for the decoupling controller.

Post-Compensator: $W(s) = \frac{1}{h} \begin{bmatrix} \cos(-\theta) & -\sin(-\theta) \\ \sin(-\theta) & \cos(-\theta) \end{bmatrix}$

Decoupled System: $G_p(s) = G_n(s)(I + \Delta(s, \Delta\omega))$

$$G_n(s) = W(s)G_n(s) = \frac{1}{\tau_p s + 1} \begin{bmatrix} 1 & 0 \\ 0 & 1 \end{bmatrix}$$

Abstract - The front end of Los Alamos Neutron Science Center (LANSCCE) linear accelerator (linac) uses four 201.25-MHz Drift-Tube Linac (DTL) modules to accelerate the H^+ and H^- beams to 100 MeV. Three of the 201.25-MHz DTL tanks, Modules 2, 3, and 4, are powered by diacodes and the first DTL tank, module 1, is powered by a tetrode. A 20-kW solid-state power amplifier (SSPA) is used to provide ~15 kW of drive power to the tetrode. The SSPA is water-cooled and consists of 24 push-pull LDMOS transistors operating at 45% of their power saturation capability, providing ample power headroom and excellent linearity. However, the phase of the SSPA is perturbed at ± 20 degrees over a few ten minutes partially caused by the temperature dependent phase variation of the air-cooled SSPA driver circulator. This phase variation consumes most of the phase control margin of the cavity field feedback controller. In order to mitigate the effect of the SSPA's phase variation on the cavity field control, a disturbance observer has been designed and implemented on the cavity field control FPGA, which functions in parallel with the cavity field feedback controller. In this paper, the disturbance observer design and functions as well as its short- and long-term performance are described.

IV. High Power RF Amplifiers

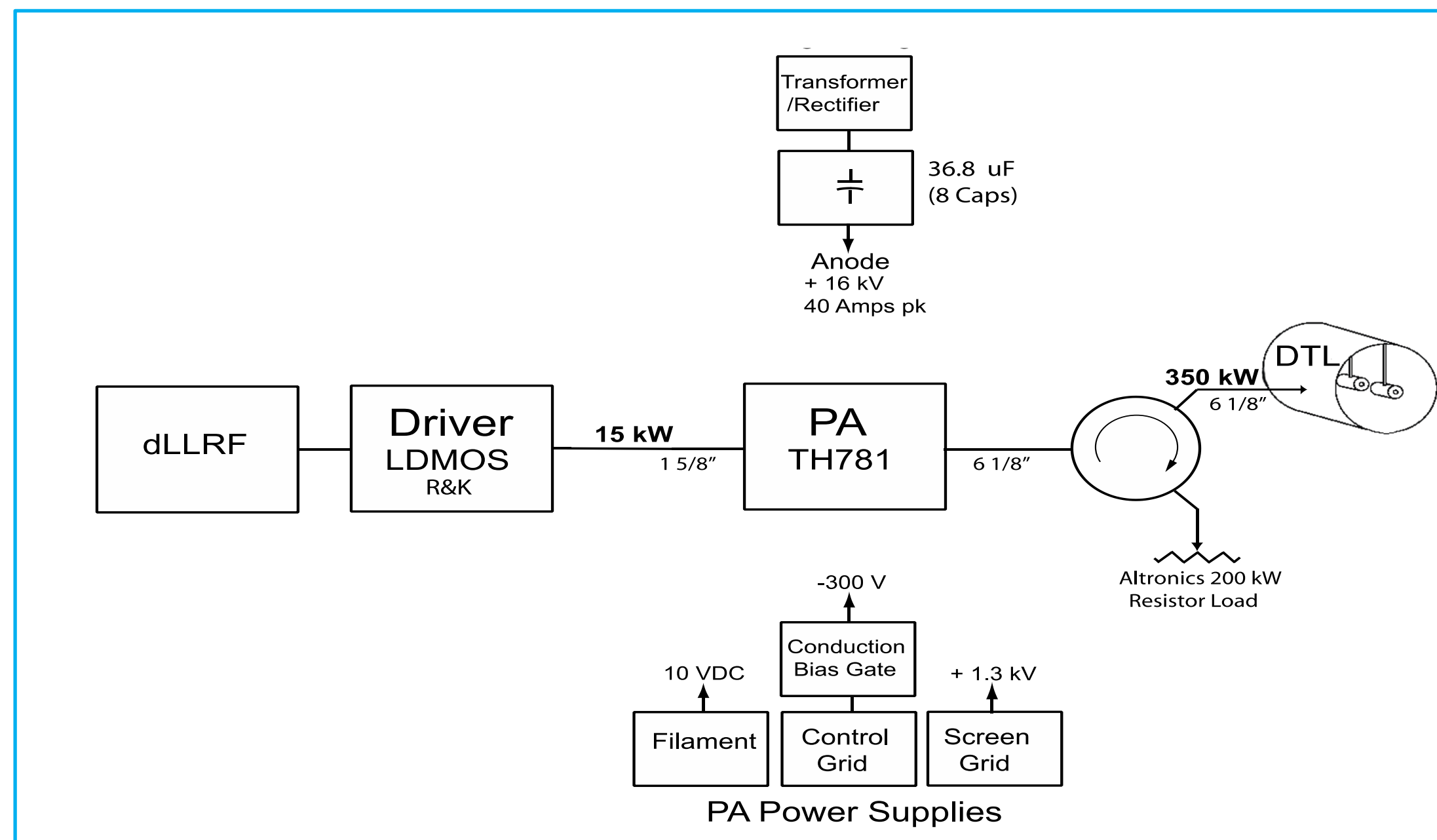


Figure 3. Diagram of New RF Amplifier System of DTL Tank1 at LANSCE LINAC

The **Thales TH781 tetrode** operates in a cavity amplifier circuit provided by the same company. It is similar to the penultimate stage in the three previously upgraded DTL RF sources but with a larger 6-1/8 inch output and 1-5/8 inch input connections. Tube lifetime averages 47K hours for the TH781 at LANSCE, considered excellent for power grid tubes. In this application we expect shorter filament emission life with higher peak cathode current, but with acceptable operation having the matched load of a circulator.

A **20 kW SSA** from R&K Company provides ~15 kW of power to the tetrode final PA. This compact amplifier is water cooled, and consists of eight 3 kW pallets, each combining four **MRF1K50H LDMOS transistors** from NXP. The pallet outputs are combined in a 8-way radial coaxial combiner. The 24 push-pull LDMOS transistors operate at 45% of their saturated capability, so there is ample headroom and good linearity. The SSA power gain is 46 dB, and it is driven from a 500 milliwatt preamplifier in the LLRF rack [John Lyles, et al., TUPA59, NAPAC2022].

Problem: A slow degradation of stability in the LLRF PI controller was discovered during the first 30 minutes of RF system warm up. It would lead to severe overshoot when the PI loops locked at the start of flat top in each RF pulse. This overshoot delayed beam start time and caused reflected power faults. Using an independent pulsed phase measurement technique, we found that a slow phase change inside the SSA gradually destabilized the LLRF loop. It shifted more than 20 degrees of RF phase, to the edge of the phase margin of the PI controller. In order to solve this problem, we implemented a Disturbance Observer Controller (DOBC) on the LLRF DSP, essentially a slow phase controller to normalize and hold the plant (amplifiers) phase within limits.

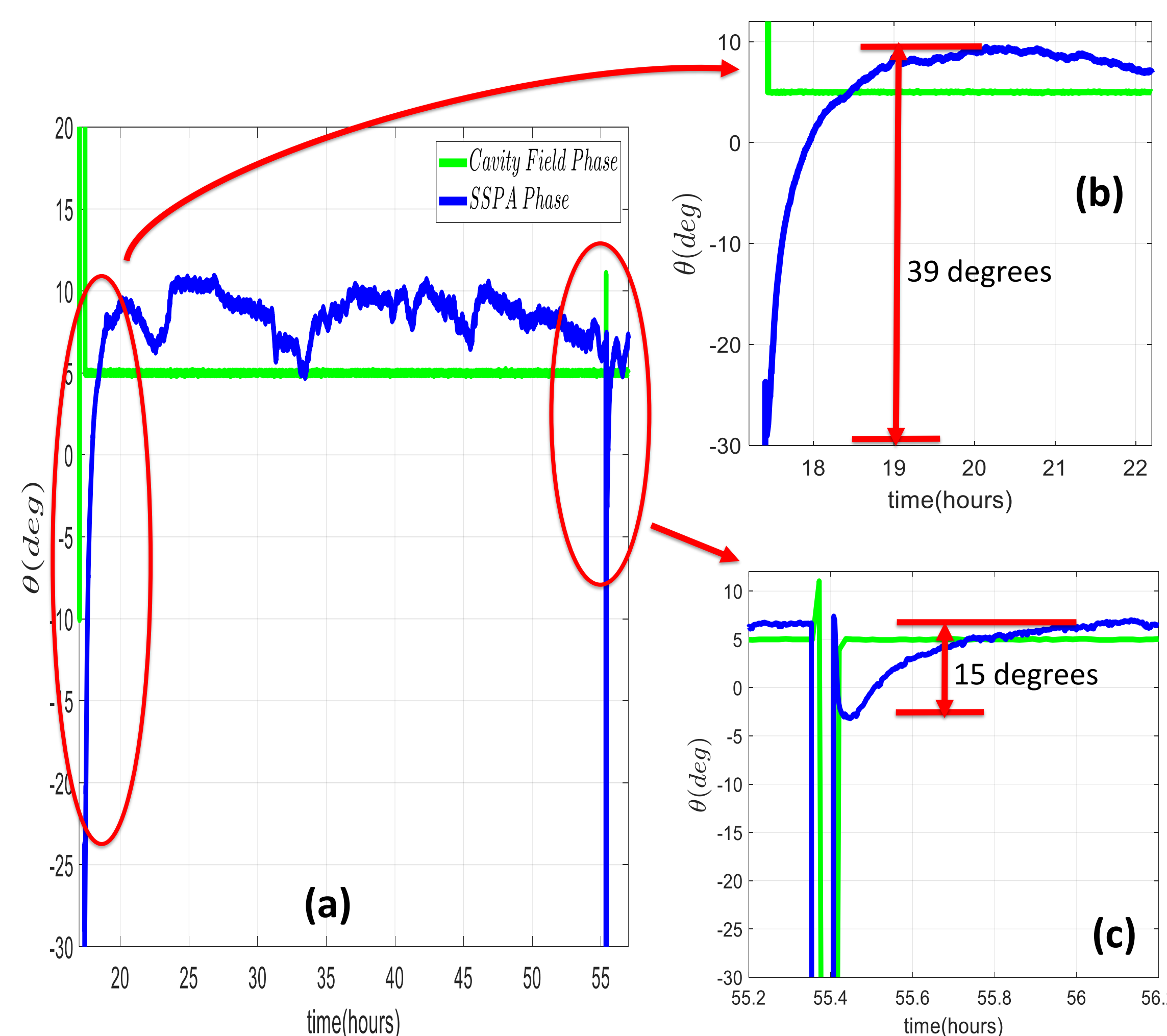


Figure 4. Phase drift observation of the SSPA. Data was captured at the middle of the RF 1000 usec RF gate pulse (a) Longterm (42 hours) Phase drift. (b) SSPA Phase drift monitored where the RF was recovered from a few hours Turn Off. SSPA was fully cool down. For 40 mins of phase drift transient, phase change was 39 degrees. (c) Phase drift monitored where the RF was recovered from the short term (<20 mins) RF trip. In both cases, DOBC increased the phase control margin of the PI feedback controller so that the Cavity Field Phase remained stabilized.

V. Disturbance Observer Controller (DOBC)

Input-Output Model for SSA :

$$\begin{bmatrix} I_{SSA}(t) \\ Q_{SSA}(t) \end{bmatrix} = H_{SSA}(s) \left\{ \begin{bmatrix} u_I(t) \\ u_Q(t) \end{bmatrix} + \begin{bmatrix} d_I(t) \\ d_Q(t) \end{bmatrix} \right\}$$

SSA I/Q Estimates by DOB:

$$\begin{bmatrix} \hat{d}_I(t) \\ \hat{d}_Q(t) \end{bmatrix} = Q_{ob}(s) H_n^{-1}(s) \begin{bmatrix} y_I(t) \\ y_Q(t) \end{bmatrix} - Q_{ob}(s) \begin{bmatrix} u_I(t) \\ u_Q(t) \end{bmatrix}$$

Nominal Plant:

$$H_n(s) = \frac{h_{SSA}}{\tau_{SSA}s + 1} \begin{bmatrix} \cos(\theta_{SSA}) & -\sin(\theta_{SSA}) \\ \sin(\theta_{SSA}) & \cos(\theta_{SSA}) \end{bmatrix}$$

	Amplitude	Phase
disturbance	$A_d = \sqrt{\hat{d}_I^2 + \hat{d}_Q^2}$	$\theta_d = \tan^{-1}\left(\frac{\hat{d}_Q}{\hat{d}_I}\right)$
estimate	$\hat{A}_d = \sqrt{\hat{d}_I^2 + \hat{d}_Q^2}$	$\hat{\theta}_d = \tan^{-1}\left(\frac{\hat{d}_Q}{\hat{d}_I}\right)$

DOB estimates the disturbance d_I and d_Q . The DOB needs the inverse model of the plant. The nominal plant $H_n(s)$ of the SSA $H_{SSA}(s)$ can be expressed as a gain, a rotation matrix and a first order lowpass filter with the high cutoff frequency, which means the implementation of the inverse of the nominal model, H_n^{-1} on the LLRF DSP is impossible. Then, instead of H_n^{-1} , $Q_{ob}H_n^{-1}$ is implemented with the design of the disturbance observer Q -filter $Q_{ob}(s)$. Here, $Q_{ob}(s)$ is designed as a two-pole lowpass filter. The first pole is for the cancellation of the zero of H_n^{-1} . The second pole is for the first order lowpass filter characteristics of $Q_{ob}H_n^{-1}$ so that it can estimate the low frequency disturbance, $d_I(t), d_Q(t)$ and reject high frequency sensor/detector noise. In the case of our application of DOBC to suppress the phase drift of the SSPA, the cutoff frequency $Q_{ob}(s)$ is set at the same frequency of the 3dB bandwidth of the nominal cavity, 2kHz.

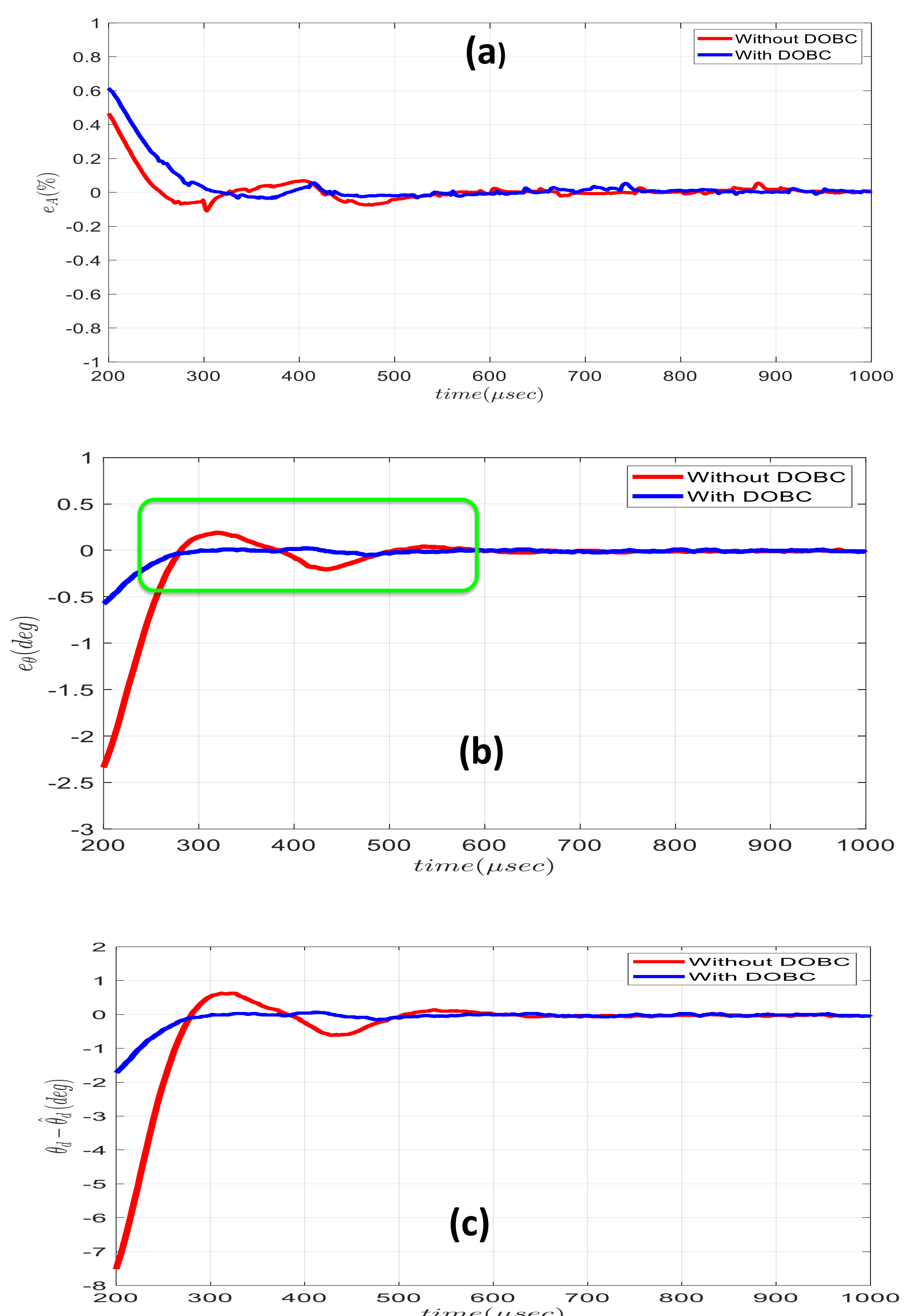


Figure 5. DOBC Performance Results of 625 usec long H+IP Beam operation for the Medical Isotope Production. The beam is on at 375 usec. (a) Cavity Field Amplitude error. (b) Cavity Field Phase error. (c) Effectual SSPA phase drift, $\theta_d - \hat{\theta}_d$. Figure (a),(b) show that the DOBC improves the amplitude and phase performances discernably at the beam loading transient. Figure (c) shows that at 200 usec, the phase error is improved 5.7 degrees. Figure (a),(b) also shows that the beam pulse length can be elongated from 625 usec to 750 usec satisfying the error requirements of LANSCE LINAC.